Automated Localization of the Seizure Focus using Interictal Intracranial EEG

Jing Jin[1], Justin Dauwels[2], and Sydney Cash[3]

Abstract— **Up to 30% of epileptic patients have seizures poorly controlled with anti-epileptic drugs alone. Surgical therapy might be beneficial to patients who respond poorly to drug treatments. It is therefore crucial to accurately localize the seizure focus. Neurologists rely heavily on seizures to determine the focus. The invasive recordings usually continue for days or weeks, which is costly and entails significant risk for the patients.**

In this paper, techniques are developed to localize the seizure focus using brief interictal intracranial EEG (iEEG). A supervised learning paradigm is utilized making use of features extracted from interictal iEEG on multiple referential montages. Analysis of 14 epileptic patients (implanted with depth electrodes) shows that iEEG features such as slowing, ripples, spikes, and local synchrony measures are strongly correlated to the seizure focus. These procedures may allow reliable localization of the seizure focus from brief interictal iEEG, which in turn may lead to shorter hospitalizations.

I. INTRODUCTION

Epilepsy is a group of chronic disorders of the brain, which are characterized by unprovoked recurrent seizures. Around 50 million people worldwide have epilepsy, and only 70% of newly diagnosed epilepsy can be successfully controlled with anti-epileptic drugs [1]. Surgical therapy is often beneficial to patients who respond poorly to drug treatments. Regional resection may provide seizure reduction or even cure [2]. The success of surgical resection strongly depends on accurate localization of the seizure focus. Apart from medical imaging modalities such as MRI and SPECT, modern clinical practices utilize EEG (scalp or intracranial) for localizing the surgical seizure focus [3]. Intracranial EEG (iEEG) is only necessary for intractable cases when scalp EEG is non-conclusive. On the other hand, neurologists rely heavily on EEG containing seizures to determine the focus. However, due to the unprovoked and infrequent natures of seizures, the invasive recordings usually continue for days or weeks until enough seizures are captured.

In this paper, brief interictal iEEG recordings are used to determine the seizure focus. Our analysis shows that interictal iEEG recordings do contain significant relevant information about the seizure focus. In the long term, instead of seizure EEG, neurologists may rely on brief interictal iEEG to delineate the seizure focus. It would drastically reduce the time of hospitalization for intractable epileptic patients. In addition, majority of the current localization studies are about scalp EEG, and iEEG recorded with surface electrodes. In this paper, we specifically consider iEEG recorded by means of depth electrodes.

The problem of localizing electrodes inside the seizure focus can be considered as binary classification. Several studies have suggested that both univariate and multivariate analysis may help to delineate epileptogenic cortex [4], [5]. In earlier work [2], [6], we have combined univariate feature such as slowing, and multivariate features such as Pearson correlation coefficient [7], magnitude coherence [7], phase synchrony [8], and omega complexity [9], for the purpose of localizing the seizure focus from interictal iEEG. In this paper, building upon our earlier results, we include two more univariate features, i.e., ripples [10], and interictal spikes [11], in combination with slowing, cross-correlation coefficient and phase synchrony, to localize the seizure focus. We also consider more patients (14 instead of 5).

A supervised learning paradigm is utilized in which the clinical determinations of seizure focus are used for training together with input features. Specifically, an adaptive boosting algorithm [12] was applied to test all possible combinations of features. Our numerical results have shown that combining features results in more accurate predictions. However, adding more features does not seem to always improve the performance. In the combination of features with best classification performance (spikes and phase synchrony on local common average montage, and ripples on global common average montage), the accuracy is $\geq$80% for 11 of 14 patients.

This paper is organized as follows. In section II, we briefly explain our interictal iEEG data and techniques for signal processing. In section III, we present our numerical results, and in section IV, we offer concluding remarks.

II. METHODS

In this section, we briefly explain the interictal iEEG data analyzed in this paper. We also discuss how we preprocessed the iEEG signals, besides the binary classification procedure, and the iEEG features considered in this study.

A. Epileptic Interictal Intracranial EEG

14 drug-resistant patients with focal epilepsy underwent depth electrode implantation at Massachusetts General Hospital. The position of the electrodes was selected exclusively for clinical reasons. In each case, multiple 1-hour recordings at least 24 hours away from seizures were analyzed. Neurophysiologists defined the seizure focus as the area showing

[1]J.Jing is with School of Electrical and Electronic Engineering, Nanyang Technological University, Singapore jing0006@e.ntu.edu.sg

[2]J.Dauwels is with School of Electrical and Electronic Engineering, Nanyang Technological University, Singapore justin@dauwels.com

[3]S.Cash is with the Neurology Department, Massachusetts General Hospital, Boston, MA, USA, and Harvard Medical School, Cambridge, MA, USAscash@partners.org

978-1-4244-7929-0/14/$26.00 ©2014 IEEE

the first ictal activity in the seizure iEEG, which was carried out independently from this study.

The iEEG recordings have a sampling rate of 500Hz, and were band-pass filtered between 1 and 200Hz. A notch filter was applied as well to remove the 60Hz power-line interference. Before computing features, each EEG signal was normalized (mean subtracted, divided by standard deviation). In addition, the EEG analysis was performed on 3 different referential montages, including mono-polar, local common average (average of local contacts of the same electrode), and global common average (average of all the contacts of the same patient). Each depth electrode contains multiple contacts (6 or 8). For each univariate feature, the average among feature values of local contacts was used as the representative for a given electrode. For pairwise synchrony features, the average of feature values of all pairs of local contacts was used for a given electrode. The features varied considerably across patients necessitating a normalization procedure. We further divide each electrode-wise feature by the average of feature values of all the electrodes for a given record.

B. Adaptive Boosting

In this study, the binary adaptive boosting algorithm (AdaBoost) was applied as the classifier to delineate the seizure focus. AdaBoost is a general method for generating a strong classifier out of a pool of weak classifiers [12]. The weak classifiers are trained sequentially, and for classifier with index m, AdaBoost computes the weighted classification error:

$$\varepsilon_m = \sum_{n=1}^{N} d_n^{(m)} \mathcal{I}(y_n \neq h_m(x_n)), \tag{1}$$

with x_n denoting the observation, y_n the desired label, h_m the predicted label, $\mathcal{I}$ the indicator function, and $d_n^{(m)}$ the weight of observation. AdaBoost then increases the weights for misclassified observations while reducing the weights of correctly classified ones. Training of AdaBoost can be viewed as stage-wise minimization of the exponential loss:

$$\sum_{n=1}^{N} w_n \exp(-y_n f(x_n)), \tag{2}$$

with w_n denoting the normalized observation weights, $f(x) = \sum_{m=1}^{M} \alpha_m h_m(x)$ the prediction score for new data, and $\alpha_m = 0.5 \log \frac{1-\varepsilon_m}{\varepsilon_m}$ the weights of the weak predictions.

C. iEEG Features

In this paper, we explore iEEG features such as ripples, interictal spikes, slowing, cross-correlation coefficient, and phase synchrony. A novel method has been developed for ripple detection.

1) ***High Frequency Oscillations****:* High Frequency Oscillations (HFOs) are special EEG patterns recorded from intracranial electrodes in patients with intractable epilepsy (see Fig. 1a). According to frequency range, HFOs are further divided into 3 subcategories, referred to as ripples (80-250Hz), fast ripples (250-500Hz) and very fast ripples (>500Hz). HFOs can be characterized by oscillations of at least 4 cycles, with a typical duration of 80-100ms for ripples, and 30-50ms for fast ripples [13]. HFOs are believed to be associated with the seizure focus [10], with higher rates of HFOs observed in the seizure focus from interictal iEEG [14].

Given the lack of a complete definition, subjectivity is inevitable, sometimes resulting in poor agreement among reviewers. In addition, manually marking HFOs is highly time-consuming [10]. Therefore, we aim to develop an automated HFO detector. Due to the small sampling rate (500Hz), only ripples are of our interest for this study. Accordingly, each iEEG channel was high-pass filtered at 80Hz. The ripple detector utilized consists of 3 major techniques:

- ***Envelope detection via Hilbert Transform***
  The envelope $\widehat{x}$ (see Fig. 1a) of a given time series x can be obtained via Hilbert Transform [15]:
  $$\widehat{x}(t) = |x(t) + i(\frac{1}{\pi} P \int_{-\infty}^{\infty} \frac{x(\tau)}{t-\tau} d\tau)|. \tag{3}$$
  Morphological features such as amplitude and duration are well reserved by the envelope $\widehat{x}$.
- ***Thresholds on amplitude and duration***
  According to definition in [13], only waveforms with amplitude larger than 5 multiples of the standard deviation σ_n of the current input signal x_n, and duration within 80-100ms, are considered as HFOs.
- ***Iterative Process***
  The detection process is iterative as shown in Fig. 1b, such that HFOs newly detected in current stage H_n are removed from the previous input signal x_n, to initiate the new loop of detection. The iteration stops when there are no more HFOs newly detected. Iterations can help to reduce the false negatives due to small-amplitude HFOs. By removing HFOs iteratively, the remaining signal left is the baseline (without HFOs).

The performance of the proposed ripple detector is validated on a 30min interictal iEEG segment with total 797 HFOs manually annotated by 2 experts (85% agreement). We only considered the HFOs that were detected by both experts. On this set of labeled data, the proposed algorithm achieves 97% accuracy, and a running time of 33s.

2) ***Interictal Spikes****:* Interictal spikes are brief, morphologically defined events observed in EEG of patients with epilepsy [11] (see Fig. 1c). Interictal spikes are highly correlated with epilepsy and may potentially be used for diagnostic purpose [16], [17]. In order to detect the interictal spikes for each EEG channel, we apply the non-linear energy operator (NLEO) widely used to estimate the energy content of a linear oscillator in AM-FM modulation. Due to its accentuation of high frequencies and computational efficiency, NLEO is believed to be an effective spike detector in biomedical signal processing [18]. The NLEO of discrete-time series $x(t)$ is defined as:

$$\Psi(x) = x^2(n) - x(n+1)x(n-1). \tag{4}$$

NLEO is further smoothed by a Gaussian kernel to achieve sufficient reduction of interference without loosing much

Feature	Mono-polar			Local Common Average			Global Common Average		
	Focus	Normal	p-values	Focus	Normal	p-values	Focus	Normal	p-values
	mean±std	mean±std		mean±std	mean±std		mean±std	mean±std	
slowing	1.09±0.20	0.97±0.13	1.3E-12	1.05±0.16	0.98±0.13	5.7E-07	1.05±0.16	0.98±0.13	9.5E-05
HFO	1.61±1.63	0.70±0.81	1.5E-09	2.00±1.67	0.68±1.00	2.4E-20	1.77±1.11	0.76±0.79	1.0E-20
spike	1.44±2.03	0.73±1.04	2.73E-04	1.66±1.22	0.79±0.73	1.1E-12	1.51±0.98	0.84±0.79	2.77E-11
xCorr	1.23±17.16	0.93±21.19	0.44	-11.37±134	4.9±172.83	0.11	233.54±5270	-72.25±1692	0.45
phase	0.90±0.25	1.03±0.26	4.3E-06	0.90±0.31	1.03±0.34	5.5E-05	0.87±0.31	1.04±0.34	1.8E-06

TABLE I: Statistic characteristics of (normalized) iEEG features.

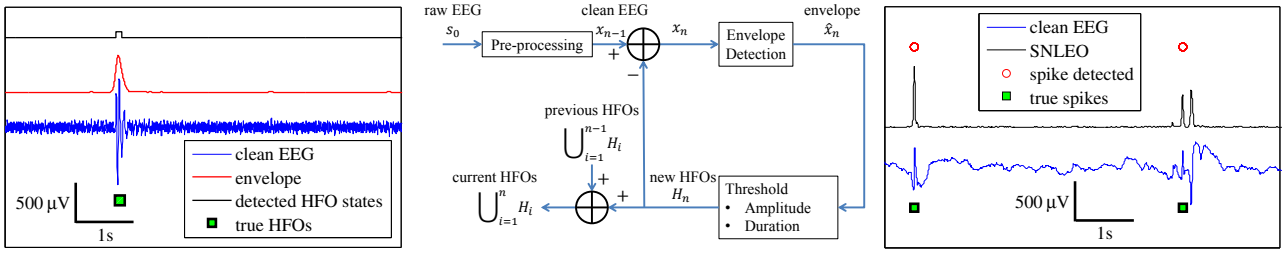

(a) (b) (c)

Fig. 1: (a) HFO with envelope obtained via Hilbert Transform, (b) Block diagram of the proposed ripple detector, and (c) Interictal spike detection via Smoothed NLEO.

time resolution. At last, a hard threshold is applied, where the threshold value is equal to 5 times the mean of the smoothed NLEO output $\widetilde{\Psi}(x)$ [19]. Consequently, only sufficiently large peaks associated with local maxima are kept, corresponding to spikes starting with rising flanks (see Fig.1c).

*3) **Slowing and Local Synchrony**:* iEEG signals recorded from damaged cortex often seem to be "slower", i.e., containing more power at low frequencies [2]. Relative power is used to quantify this slowing effect by computing the ratio of power from [1 8Hz] to that from the entire band [1 200Hz]. Pairwise cross-correlation and Hilbert phase [8] are computed to quantify magnitude and phase synchrony respectively.

D. Sensitivity and Specificity

Sensitivity relates to the test's ability to identify a condition correctly, while specificity relates to the test's ability to exclude a condition correctly [20]. With the confusion matrix

		Ground Truth	
		Positive	Negative
Test Outcomes	Positive	a	b
	Negative	c	d

TABLE II: Confusion matrix of a test.

shown in Tab. II, sensitivity and specificity are computed as:

$$sensitivity = \frac{a}{a+c}, \quad specificity = \frac{d}{b+d}. \qquad (5)$$

III. Results

The statistical characteristics of the iEEG features and p-values of Mann-Whitney tests are summarized in Tab. I, with boxplots shown in Fig. 2. AdaBoost was applied to test all possible combinations of features. In each case, the classification rate, sensitivity and specificity (consider channels inside the focus as positive) were computed through leave-one-patient-out cross-validation. Results for increasing no. of features are shown in Tab. III. Combining features results in more accurate predictions, however adding more features does not seem to improve the performance. By contrast, for more than 4 features, the performance gradually starts

Features	Err	Sens	Spec
HFO_3	21%	70%	83%
$phase_2$-HFO_3	14%	64%	93%
$spike_2$-$phase_2$-HFO_3	**14%**	**69%**	**93%**
$spike_2$-$phase_2$-HFO_2-HFO_3	15%	67%	92%
$slowing_1$-$xCorr_2$-$phase_2$-$spike_2$-HFO_3	15%	71%	89%
$d = 6$	16%	71%	87%
$d = 7, 8$	19%	56%	88%
$d = 9$	20%	56%	87%
$d = 10, 11, 12$	17%	59%	90%
$d = 13$	17%	65%	89%
$d = 14$	17%	59%	90%
$d = 15$ (All)	19%	60%	88%

TABLE III: Classification results for increasing no. of features d (the best combination only), and indices 1, 2, 3 referring to different referential montages, i.e., mono-polar, local common average, and global common average respectively.

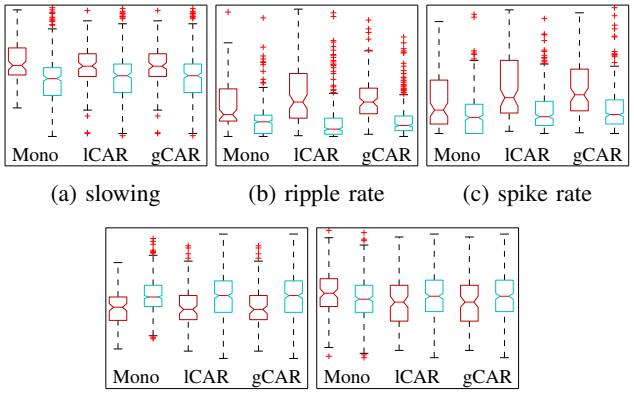

(a) slowing (b) ripple rate (c) spike rate

(d) Hilbert phase (e) x-Correlation

Fig. 2: Boxplots of (normalized) iEEG features, with red boxes referring to electrodes inside the seizure focus, blue boxes referring to channels outside the focus ("normal"), and "Mono", "lCAR", "gCAR" referring to different referential montages, i.e., mono-polar, local common average, and global common average respectively.

deteriorating, probably due to overfitting [2], [21]. In Tab. IV, we list results for individual records from different patients. Due to space constraints, we limit ourselves to results with the most discriminative combination of features (see Tab. III). Out of 14 patients, there are 11 cases having accuracy $\geq$80%. The performance varies across patients: in the best cases (P1, 3, 13, and 14), the classification accuracy is 100%, while for some cases (P2, 5, and 10), the classification sensitivity is very low. In addition, our results seem to be similar for periods where the patient is awake or asleep.

spike$_2$-phase$_2$-HFO$_3$					
Patient	**Record**	**State**	**Err**	**Sens**	**Spec**
P1	1	asleep	0%	100%	100%
	Average		**0%**	**100%**	**100%**
P2	1	awake	20%	0%	100%
	2	asleep	20%	0%	100%
	Average		**20%**	**0%**	**100%**
P3	1	asleep	0%	100%	100%
	2	awake	0%	100%	100%
	3	asleep	0%	100%	100%
	4	awake	0%	100%	100%
	5	awake	0%	100%	100%
	6	asleep	0%	100%	100%
	Average		**0%**	**100%**	**100%**
P4	1	awake	0%	100%	100%
	2	asleep	0%	100%	100%
	3	awake	20%	50%	100%
	4	asleep	0%	100%	100%
	Average		**5%**	**88%**	**100%**
P5	1	awake	60%	0%	80%
	2	asleep	60%	0%	80%
	3	awake	30%	40%	100%
	4	asleep	60%	0%	80%
	Average		**53%**	**10%**	**85%**
P6	1	awake	10%	50%	100%
	2	asleep	0%	100%	100%
	3	awake	20%	50%	88%
	4	asleep	0%	100%	100%
	Average		**8%**	**75%**	**97%**
P7	1	asleep	20%	50%	88%
	2	awake	30%	0%	88%
	3	asleep	20%	50%	88%
	Average		**22%**	**33%**	**88%**
P8	1	awake	20%	50%	88%
	2	asleep	20%	50%	88%
	3	asleep	20%	50%	88%
	Average		**20%**	**50%**	**88%**
P9	1	awake	0%	100%	100%
	2	asleep	17%	100%	75%
	3	awake	0%	100%	100%
	4	asleep	0%	100%	100%
	Average		**4%**	**100%**	**94%**
P10	1	awake	30%	0%	78%
	2	asleep	50%	0%	56%
	3	awake	50%	0%	56%
	Average		**43%**	**0%**	**63%**
P11	1	awake	20%	0%	100%
	2	asleep	20%	0%	100%
	3	awake	20%	100%	75%
	4	asleep	20%	100%	75%
	Average		**20%**	**50%**	**88%**
P12	1	awake	14%	100%	80%
	2	asleep	0%	100%	100%
	3	awake	14%	100%	80%
	4	asleep	0%	100%	100%
	Average		**7%**	**100%**	**90%**
P13	1	awake	0%	100%	100%
	2	asleep	0%	100%	100%
	3	awake	0%	100%	100%
	4	asleep	0%	100%	100%
	Average		**0%**	**100%**	**100%**
P14	1	awake	0%	100%	100%
	2	asleep	0%	100%	100%
	3	awake	0%	100%	100%
	4	asleep	0%	100%	100%
	Average		**0%**	**100%**	**100%**

TABLE IV: Classification results for individual records obtained by AdaBoost algorithm, with the best feature combination in Tab. III.

IV. CONCLUSIONS

In this paper, techniques were proposed to automatically localize the seizure focus using brief interictal intracranial EEG recorded by depth electrodes, by exploiting various iEEG features. To further improve this approach, we will investigate in depth the few cases where the current algorithm fails to localize the seizure focus. Including additional iEEG features may potentially lead to better results.

REFERENCES

[1] World Health Organization, "Epilepsy Fact Sheet N°999," *WHO, http://www.who.int/mediacentre/factsheets/fs999/en/index.html*, 2012.

[2] J. Dauwels, E. Eskandar, A. Cole, D. Hoch, R. Zepeda, and S. S. Cash, "Graphical models for localization of the seizure focus from interictal intracranial EEG," in *Acoustics, Speech and Signal Processing (ICASSP), 2011 IEEE International Conference on*, pp. 745–748, IEEE, 2011.

[3] P. Jayakar, M. Duchowny, T. J. Resnick, and L. A. Alvarez, "Localization of seizure foci: pitfalls and caveats," *Journal of Clinical Neurophysiology*, vol. 8, no. 4, pp. 414–431, 1991.

[4] T. Akiyama, B. McCoy, C. Y. Go, A. Ochi, I. M. Elliott, M. Akiyama, E. J. Donner, S. K. Weiss, O. C. Snead, J. T. Rutka, *et al.*, "Focal resection of fast ripples on extraoperative intracranial EEG improves seizure outcome in pediatric epilepsy," *Epilepsia*, vol. 52, no. 10, pp. 1802–1811, 2011.

[5] D. W. Kim, H. K. Kim, S. K. Lee, K. Chu, and C. K. Chung, "Extent of neocortical resection and surgical outcome of epilepsy: intracranial EEG analysis," *Epilepsia*, vol. 51, no. 6, pp. 1010–1017, 2010.

[6] J. Dauwels, E. Eskandar, and S. Cash, "Localization of seizure onset area from intracranial non-seizure EEG by exploiting locally enhanced synchrony," in *Engineering in Medicine and Biology Society, 2009. EMBC 2009. Annual International Conference of the IEEE*, pp. 2180–2183, IEEE, 2009.

[7] P. L. Nunez and R. Srinivasan, *Electric fields of the brain: the neurophysics of EEG*. Oxford university press, 2006.

[8] J.-P. Lachaux, E. Rodriguez, J. Martinerie, F. J. Varela, *et al.*, "Measuring phase synchrony in brain signals," *Human brain mapping*, vol. 8, no. 4, pp. 194–208, 1999.

[9] N. Saito, T. Kuginuki, T. Yagyu, T. Kinoshita, T. Koenig, R. D. Pascual-Marqui, K. Kochi, J. Wackermann, and D. Lehmann, "Global, regional, and local measures of complexity of multichannel electroencephalography in acute, neuroleptic-naive, first-break schizophrenics," *Biological psychiatry*, vol. 43, no. 11, pp. 794–802, 1998.

[10] R. Zelmann, M. Zijlmans, J. Jacobs, C. E. Châtillon, and J. Gotman, "Improving the identification of high frequency oscillations," *Clinical Neurophysiology*, vol. 120, no. 8, pp. 1457–1464, 2009.

[11] H. Gastaut and R. J. Broughton, *Epileptic seizures: clinical and electrographic features, diagnosis and treatment*. Thomas Springfield (IL):, 1972.

[12] Y. Freund and R. E. Schapire, "A desicion-theoretic generalization of on-line learning and an application to boosting," in *Computational learning theory*, pp. 23–37, Springer, 1995.

[13] J. Jacobs, P. LeVan, R. Chander, J. Hall, F. Dubeau, and J. Gotman, "Interictal high-frequency oscillations (80–500 Hz) are an indicator of seizure onset areas independent of spikes in the human epileptic brain," *Epilepsia*, vol. 49, no. 11, pp. 1893–1907, 2008.

[14] E. Urrestarazu, R. Chander, F. Dubeau, and J. Gotman, "Interictal high-frequency oscillations (100–500 Hz) in the intracerebral EEG of epileptic patients," *Brain*, vol. 130, no. 9, pp. 2354–2366, 2007.

[15] S. L. Hahn, *Hilbert transforms in signal processing*, vol. 2. Artech House Boston, 1996.

[16] J. Engel, *Seizures and epilepsy*, vol. 83. Oxford University Press, 2013.

[17] K. Staley, J. L. Hellier, and F. E. Dudek, "Do interictal spikes drive epileptogenesis," *The Neuroscientist*, vol. 11, no. 4, pp. 272–276, 2005.

[18] S. Mukhopadhyay and G. Ray, "A new interpretation of nonlinear energy operator and its efficacy in spike detection," *Biomedical Engineering, IEEE Transactions on*, vol. 45, no. 2, pp. 180–187, 1998.

[19] P. Maragos, J. F. Kaiser, and T. F. Quatieri, "On amplitude and frequency demodulation using energy operators," *Signal Processing, IEEE Transactions on*, vol. 41, no. 4, pp. 1532–1550, 1993.

[20] D. G. Altman and J. M. Bland, "Diagnostic tests 1: Sensitivity and specificity," *BMJ: British Medical Journal*, vol. 308, no. 6943, p. 1552, 1994.

[21] R. O. Duda, P. E. Hart, and D. G. Stork, *Pattern classification*. John Wiley & Sons, 2012.